

Quantum Chaos with Nonperiodic, Complex Orbits in the Resonant Tunneling Diode

D. S. Saraga and T. S. Monteiro

*Department of Physics and Astronomy, University College, University of London, Gower Street,
London WC1E 6BT, United Kingdom*

(Received 8 June 1998)

We show that special types of orbits, which are *nonperiodic* and *complex* “saddle orbits” (SOs), describe accurately the quantal and experimental current oscillations in the resonant tunneling diode in tilted fields. The SOs solve the puzzle of broad regions of experimental oscillations where we find no real or complex periodic orbit (PO) that can explain the data. The SOs succeed in regimes involving several nonisolated POs, where PO formulas fail. We show that their contribution can, unexpectedly, decay very slowly in the classical limit. [S0031-9007(98)07876-4]

PACS numbers: 05.45.+b, 03.65.Sq, 73.20.Dx

The resonant tunneling diode (RTD) in tilted fields has recently been intensively investigated as an experimental probe of “quantum chaos” [1–6]. It is widely considered to be a paradigm of periodic orbit (PO) theory in a real system, yet to date no PO formula has been shown to provide a full and quantitative description of the current. Several approaches were presented recently [7–9], expressing the tunneling current in terms of periodic orbits. We demonstrated previously [10] that they yielded only reasonable agreement for the *amplitudes* of current oscillations in specific regimes, namely, the stable (torus-quantization) region and its opposite extreme, the isolated unstable periodic orbit regions. They failed in an intermediate regime spanning a broad range of field values. There one finds regions where there is no real PO or alternatively competing nonisolated POs. As we argue below, it is not simply a question of improving the PO theory with uniform approximations. In the regions where there is no real PO, even complex “ghost” POs [11] cannot explain the experimental oscillations (for convenience we continue nevertheless to refer to these regions as “ghost regions”).

While the well-known Gutzwiller trace formula relates classical POs to the quantal density of states (DOS) of a chaotic system, in our case, we seek a semiclassical theory for the DOS *weighted* by a matrix element (here a tunneling probability). Previous semiclassical theories of matrix elements for e.g., molecular vibrational spectra [12] excluded the matrix element from stationary phase considerations imposed on the rapidly varying function $e^{iS(z,z')/\hbar}$ of the classical action S of a trajectory. This approach yields the observed spectra as a sum over POs. However, in the RTD problem, the tunneling matrix element varies on a comparable scale to $S(z, z')/\hbar$. We show here that the correct stationary phase condition including the tunneling matrix element, arising from the theory proposed in [8], yields orbits of a new type—which we call “saddle orbits” (SOs). The SOs are *nonperiodic* and *complex* and describe the current accurately even in regimes where the previous semiclassical PO theories failed. They also show good agreement with the experimental amplitudes obtained from Bell Lab data [2]. The

SOs are quite distinct from the real closed orbits identified in atomic photoabsorption from localized ground states [13]. As for ghosts, the imaginary component of the action provides a damping term. We show that for SOs a further weighting term due to the matrix element can partially cancel this damping. This yields contributions which can decay slowly with decreasing \hbar , also solving the puzzle of oscillations which persist far into the ghost regions.

We recall briefly the RTD model [1]. An electric field F (along x) and a magnetic field B in the x - z plane (at tilt angle θ to the x axis) are applied to a double barrier quantum well of width $L = 1200 \text{ \AA}$. Because of translational invariance, the dynamics reduces to two degrees of freedom in x and z . The electrons are confined in the z direction by the magnetic field which provides a harmonic potential. In the x direction they are confined by the barriers. Electrons in a two-dimensional electron gas accumulate at the first barrier and tunnel through both barriers giving rise to a tunneling current I . In the process they probe the classical dynamics—regular or chaotic—within the well. The current oscillates as a function of applied voltage V . After rescaling with respect to B ($q \rightarrow q, p \rightarrow p/B$) [9], the dynamics at given θ and ratio of injection energy to voltage ($R = E/V \sim 0.15$ for the Bell Lab experiments) depends only on the parameter $\epsilon = V/LB^2$.

The theoretical scaled current is a DOS weighted by a tunneling matrix element: $I(B) = \sum_i W_i \delta(B - B_i)$. We used the Bardeen matrix element [14] form for W_i , which is an overlap between ϕ_0 , the initial state describing the electrons prior to tunneling, and ψ_i , the wave function in the quantum well. We consider here that the initial state is in the lowest Landau state: $\phi_0(z) = \sqrt{B \cos \theta / \pi} \exp(-B \cos \theta z^2 / 2)$.

In the experiments, incoherent processes such as phonon emission damp the current by $e^{-T/\tau}$, where T is the period of the motion of an electron in the well and $\tau \sim 0.11$ ps. Details of the experimental data reduction and quantum calculations were given in [9,10]. We can obtain reliable experimental amplitudes in regimes where

the current is dominated by a single frequency (pure period-one or period-two).

For the semiclassics, one can reexpress the Bardeen matrix element in terms of energy Green's functions and use their semiclassical expansion over classical paths to get the following expression for the tunneling current [8]:

$$I(B) \propto \text{Re} \int dz \int dz' \sum_{cl} m_{12}^{-1/2} e^{iS(z,z') - B \cos \theta (z^2 + z'^2)/2}, \quad (1)$$

where $m_{12} = \frac{\partial z'}{\partial p_z}$ is an element of the monodromy matrix m_{ij} , for a trajectory $(x = 0, z; p_x, p_z) \rightarrow (x' = 0, z'; p'_x, p'_z)$ with initial momentum p_z along z , and which must connect both walls of the well.

The stationary phase condition applied to Eq. (1) gives $i \frac{\partial S}{\partial z} - B \cos \theta z = 0 = i \frac{\partial S}{\partial z'} - B \cos \theta z'$. The contributing trajectories will therefore satisfy the condition

$$p_z = i \cos \theta z, \quad p'_z = -i \cos \theta z', \quad (2)$$

as $\frac{\partial S}{\partial z} = -B p_z$ in our scaled model. One sees clearly that these trajectories, which we call saddle orbits, will invariably be *complex* and *nonperiodic*. It follows that we cannot consider the repetitions of a given SO—as one does for POs when investigating period-doubled oscillations. Instead, one finds other SOs of quite different shapes with longer periods. We found that all the SOs which give a substantial contribution to the current have $z = z'$. They retrace themselves *once* because of an intermediate bounce normal to a wall or a “soft” bounce on the energy surface.

In [8] the term in Eq. (2) was neglected in order to get a formula in terms of POs with null momentum $p_z = 0 = p'_z$. It was found in [10] that this formula is accurate only over part of the experimental range. In order to understand over which regimes PO formulas succeed and where they fail, we consider the regime where a self-retracing SO and a PO counterpart are reasonably close. One can then establish a link between them by expressing the SO in terms of an expansion around the PO. Making a Taylor expansion of the action and neglecting $\frac{\partial^n S}{\partial z^n}$ for $n > 2$, one finds

$$z_{SO} \cong \frac{z_{PO}}{1 - \delta}, \quad (3)$$

where $\delta = i \cos \theta \frac{\bar{m}_{12}}{\bar{m}_{11} - 1}$ and \bar{m}_{ij} is the scaled monodromy matrix of the PO. Later we find that the PO and SO current amplitudes are in agreement only when this perturbative link is valid. Also, we found that non-self-retracing SOs, which correspond to segments of POs, are not relevant to these experiments.

We plot some of these trajectories in Figs. 1(a)–(d), together with their corresponding PO counterpart. The link between SOs and POs is evident in Fig. 1(a), which shows a regime where the SO and PO are very similar. In this case the x - z path of the SO is not very complex (the imaginary part is an order of magnitude smaller than

the real part). The connection between SO and PO is generally not so visible though. Figure 1(b) shows the stable PO t_0 , its related “primitive” SO t_0 -SO as well as *another* SO, which seems completely unrelated to them. This SO ($2t_0$ -SO) plays, in fact, the role of the *second repetition* of the primitive SO: its complex action and the real part of its period are twice (within 1%) those of t_0 -SO. Despite the obvious difference in their path, some of the properties of the (SO-PO) pair such as their monodromy matrix or action can be very similar.

Perhaps the most interesting situation is when Eq. (3) is not valid and there is no straightforward relation between the SOs and the POs which can contribute to the current at a given period. This is seen in Fig. 1(c), where the SO interpolates between a ghost PO and a real PO. This fact is illustrated in Fig. 1(e), where we plotted the evolution of the starting position z (at $x = 0$) against ϵ . One sees that a single SO is linked to a large number of POs. The latter are the basic traversing 2-bounce POs (t_0, t'_0, \dots) to which have been attributed (in previous work) the period-one oscillations of the current. Their complicated dynamics has been well studied [9,15]. They undergo an infinite cascade of tangent bifurcations, where they

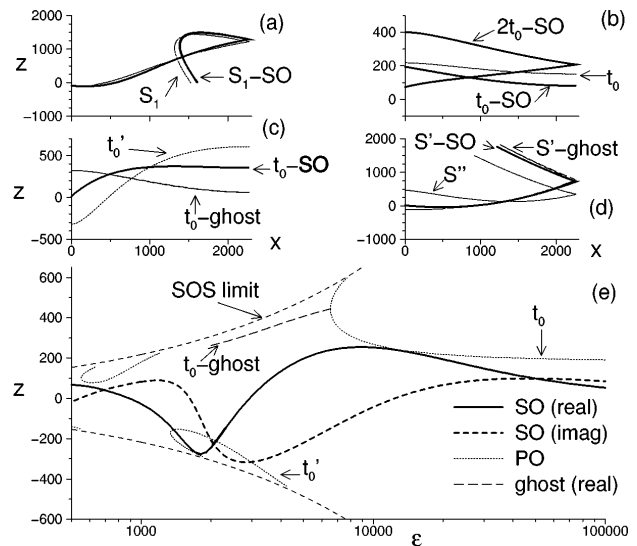


FIG. 1. (a)–(d) Shape in x - z plane of the real part of SOs, with the related POs. (a) $\theta = 27^\circ$, $\epsilon = 2000$. Differences between the SO and its counterpart PO (S_1) are minimal. (b) $\theta = 11^\circ$, $\epsilon = 20000$. We show the main period-one PO t_0 , its related SO as well as the SO which is related to its second repetition $2t_0$. (c) $\theta = 11^\circ$, $\epsilon = 3000$. The SO is between the real PO t'_0 and the ghost PO t_0 . (d) $\theta = 27^\circ$, $\epsilon = 5000$. A ghost PO (S') and a real PO (S'') are present. The real part of the SO is closer in shape to the real part of the ghost. (e) $\theta = 11^\circ$. Evolution of the starting z (at $x = 0$) with ϵ for the main period-one PO t_0 , showing part of its infinite cascade of tangent bifurcations where t_0 disappears, leaving a ghost while a similar PO appears at a lower ϵ . Also shown is the behavior of the related SO. We see that a single SO “interpolates” smoothly between the successive disappearing and reentrant POs. This illustrates the striking simplicity and power of the SO approach in comparison with POs.

disappear leaving a ghost. Subsequently at some lower ϵ a similar PO reappears from the opposite edge of the surface of section. Over some ϵ interval this reentrant PO coexists with the ghost of the old PO.

In comparison, the corresponding SO behaves in a much simpler way, “interpolating” between the successive POs. For example, for $\epsilon > 10\,000$ the SO is related to t_0 , which disappears in a tangent bifurcation at $\epsilon = 6500$. The SO remains close to the t_0 ghost down to $\epsilon = 3000$, where it veers away towards the new orbit t'_0 which appeared from the edge at $\epsilon = 4300$. One sees this fact clearly in Fig. 1(c), where the SO is between the t_0 ghost and t'_0 . The same happens at $\theta = 27^\circ$, where the 3-bounce PO S' disappears in a tangent bifurcation at $\epsilon = 7700$, leaving a ghost, while a similar PO S'' appears at $\epsilon = 5500$. As seen in Fig. 1(d), the SO is very close to the ghost of S' , but it will soon approach the new PO at lower ϵ . Note that SOs never disappear in bifurcations as they are nonperiodic, but rather when they “miss a bounce” on the emitter wall because of the voltage drop.

The semiclassical current is given by the straightforward Gaussian integration resulting from the stationary phase approximation applied on (1). After normalizing to the amplitude at $\theta = 0^\circ$, the current due to one SO is approximated by a simple analytical formula:

$$I(B) = \text{Re} \frac{e^{B(i\tilde{S} - \cos \theta z^2) + i\mu\pi/2}}{\sqrt{-\cos \theta \tilde{m}_{12} + \tilde{m}_{21}/\cos \theta + 2i\tilde{m}_{11}}}, \quad (4)$$

where μ is a Maslov index, and \tilde{S} and \tilde{m}_{ij} are, respectively, the scaled action and element of the classical monodromy matrix of the SO. One can also use the expansion in Eq. (3) to approximate the SO current by the related PO. Expanding the action S of the SO around the PO up to second order, one finds

$$I(B) \simeq \text{Re} \frac{e^{B[i\bar{S} - \cos \theta \bar{z}^2(1/1-\delta)] + i\bar{\mu}\pi/2}}{\sqrt{-\cos \theta \bar{m}_{12} + \bar{m}_{21}/\cos \theta + 2i\bar{m}_{11}}}, \quad (5)$$

where \bar{S} and \bar{z} are, respectively, the scaled action and starting position of the PO. This is exactly the PO formula presented in [8] and tested in [10]. So we see that the PO formula will give accurate results provided that the higher derivatives of S are small *and* that the perturbative expansion of the SO around the PO is justified. This latter point is the most relevant, as it is the prime reason why the PO formula fails in certain regions.

We show in Fig. 2 a comparison between quantal, experimental, and semiclassical amplitudes for period-one and period-two currents. The corresponding comparison with the PO formula was presented in [10].

Figure 2(a) shows the period-one amplitudes at $\theta = 11^\circ$ in the unstable and ghost region, while Fig. 2(b) shows the stable torus regime. We found [10] that for the stable ($\epsilon > 7000$) and the chaotic ($\epsilon < 2500$) regions PO theory (using t_0 and t'_0) gave good agreement. These are regions where the SO and PO currents are almost equal, according to Eq. (5). But the intermediate

region ($2500 < \epsilon < 7000$) was a puzzle: the PO formula including the ghost failed to account for the quantal and experimental oscillations, by a factor of 3. Figure 2(a) shows that the SO completely solves this problem, giving accurate results over the entire range from the torus regime to the chaotic regime, including the ghost region.

The main reason why Eq. (5) fails in that region was illustrated in Fig. 1(a): the SO cannot be approximated by the ghost PO, as it is also related to the new t'_0 . In this case it is not because the third derivative of S is large.

The same happens for the S' ghost at 27° [Fig. 2(d)]. The SO describes very well the broad plateau of quantal and experimental amplitudes, while POs failed. Once again, this is because the SO interpolates between the ghost (which appears at $\epsilon = 7700$) and the new PO S'' (which appears at $\epsilon = 5500$), as illustrated in Fig. 1(d). Therefore, the failure of the PO theory in these regions is due to the sequence of tangent bifurcations, each followed by a new reentrant PO [as illustrated in Fig. 1(f)], which rules out a simple connection between one SO and one PO.

The SO also solves the intricate superposition of two nonisolated (in action and phase-space localization) POs [10]: the second repetition of t_0 (which yields quantized torus states) and S' for $\epsilon \sim 13\,000$, $\theta = 27^\circ$. Indeed,

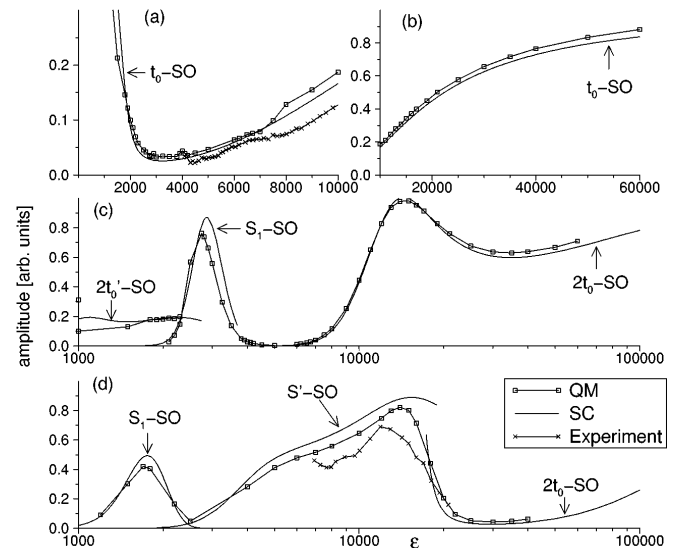


FIG. 2. Quantal, experimental, and semiclassical amplitudes. The SO labels indicate which PO they are related to. Period one at $\theta = 11^\circ$ in the unstable/ghost region (a) and in the stable (torus-quantization) regime (b). t_0 -SO describes very accurately the quantal current, even in the ghost region ($2500 < \epsilon < 7000$) where PO theories fail. (c) Period two at $\theta = 11^\circ$. The SO formula improves over the PO formula, giving very accurately the quantal maximum ($\epsilon \sim 15\,000$). Experimental amplitudes were not obtained for this case since there was a strong period-one beat in this region. (d) Period two at $\theta = 27^\circ$. As in (c), the peak at low ϵ is well described by both the SO and the PO formulas (S_1). S' -SO gives the contribution to the very broad plateau where no real PO is present ($5000 < \epsilon < 8000$). $2t_0$ -SO is responsible for the current for $\epsilon > 17\,000$, with no overlap with S' -SO.

there is no overlapping region for the related SOs, which now describe accurately the current, as shown in Fig. 2(d). In Fig. 2(c) one sees that the period doubling maximum around $\epsilon \sim 15000$ is described very precisely by the SO, an improvement over the PO results. Finally, we note that for both angles the period-two maxima at low $\epsilon \sim 2000$ are described equally well by either the PO or the SO formula. Here both trajectories (S_1 -SO and S_1) are very similar as seen in Fig. 1(a). The experimental amplitudes are lower than theory, but this is consistent with a 10% uncertainty in τ .

The strength and persistence of the contribution of these complex orbits, even in the region where the SO formula does not reduce to the PO formula (such as in the ghost regions) is quite remarkable. Usually (e.g., in the density of states or the photoabsorption spectra of atoms [11,16]), the contribution of complex ghost POs is extremely weak. They are exponentially damped away from the bifurcation (as ϵ changes), since the imaginary part of the action increases as the ghost becomes more complex. However, in the RTD the tunneling amplitude includes an additional term due to the initial state:

$$|I(B)| \propto e^{-B[\tilde{S}_I + \cos \theta(z_R^2 - z_I^2)]}, \quad (6)$$

where the subscripts I and R denote the real and imaginary parts. We see that the *imaginary* part z_I of the starting position of a SO can partly cancel the damping due to \tilde{S}_I . This is the reason why even “very” complex SOs can contribute. For instance, the S' -SO amplitude in the ghost region at $\theta = 27^\circ$ shows a broad plateau and very slow decay away from the bifurcation ($\epsilon < 7700$).

Similarly, ghost POs are exponentially damped in the classical limit $\hbar \rightarrow 0$ (which corresponds in our scaled model to $B \rightarrow \infty$). We also investigated the $\hbar \rightarrow 0$ behavior of the SO current in the ghost regions. The behavior at $\theta = 27^\circ$ is most striking. The cancellation of the argument in Eq. (6) is near perfect, so the current amplitudes decay very slowly (linearly) with B even though S_I is large. This very surprising feature is seen experimentally (see Fig. 6 of [9]). This behavior is unique to the SOs, as it has never been observed in other “tunneling”-type complex trajectories, which are strongly suppressed as S_I/\hbar increases.

We emphasize that this work is consistent with previous studies of “scarring” in the RTD. It has been found that quantum states localized near some isolated or multiple POs can dominate the tunneling [4,5]. We have also investigated wave functions and Wigner distributions. We found that in the strong scarring regions, where the relevant scarring PO is only marginally unstable [4] (e.g., for $\theta = 27^\circ$, $\epsilon = 10000$), the real part of the SO is very close to the PO—within the “ \hbar ” quantum uncertainty. This can also be the case with scars carried by ghost

POs (e.g., $\theta = 27^\circ$, $\epsilon = 7000$). This is reasonable since after all it is the bundle of classical trajectories in the *neighborhood* of POs and SOs which scars or carries the electrons. Regions like the $\theta = 11^\circ$ ghost region where the SO and PO are really different in shape do not show strong scarring by single states and the quantal current is carried by broad clusters of states.

We conclude that the SOs are a novel and successful way to approach semiclassical quantization of these types of chaotic systems. We recall that SOs arise solely from the inclusion of the initial state in the stationary phase condition. Hence one could expect SOs to be potentially relevant in the description of the expectation value of a quantal quantity (expressed as a density of states weighted by some matrix element [12]) if the observable in the matrix element is very localized and so varies as rapidly as $e^{iS/\hbar}$. Vibrational photoabsorption spectra of molecules [12] (which also involve localized Gaussians) are one example.

We are greatly indebted to E. Bogomolny and D. Rouben for invaluable help and to G. Boebinger for providing his experimental data. T. S. M. acknowledges funding from the EPSRC. D. S. S. acknowledges financial support from the TMR programme.

-
- [1] T. M. Fromhold *et al.*, Phys. Rev. Lett. **72**, 2608 (1994).
 - [2] G. Muller, G. S. Boebinger, H. Mathur, L. N. Pfeiffer, and K. W. West, Phys. Rev. Lett. **75**, 2875 (1995).
 - [3] D. L. Shepelyansky and A. D. Stone, Phys. Rev. Lett. **74**, 2098 (1995).
 - [4] E. E. Narimanov and A. D. Stone, Phys. Rev. Lett. **80**, 49 (1998).
 - [5] P. B. Wilkinson *et al.*, Nature (London) **380**, 608 (1996).
 - [6] T. S. Monteiro, D. Delande, A. J. Fisher, and G. S. Boebinger, Phys. Rev. B **56**, 3913 (1997).
 - [7] E. E. Narimanov, A. D. Stone, and G. S. Boebinger, Phys. Rev. Lett. **80**, 4024 (1998).
 - [8] E. B. Bogomolny and D. C. Rouben, Europhys. Lett. **43**, 111 (1998); Eur. Phys. J. B (to be published).
 - [9] D. S. Saraga and T. S. Monteiro, Phys. Rev. E **57**, 5252 (1998).
 - [10] D. S. Saraga, T. S. Monteiro, and D. C. Rouben, Phys. Rev. E **58**, R2701 (1998).
 - [11] M. Kus, F. Haake, and D. Delande, Phys. Rev. Lett **71**, 2167 (1993).
 - [12] B. Eckhardt *et al.*, Phys. Rev. A **45**, 3531 (1992); B. Huppert *et al.*, J. Phys. B **30**, 3191 (1997).
 - [13] M. L. Du and J. B. Delos, Phys. Rev. A **38**, 1913 (1988).
 - [14] J. Bardeen, Phys. Rev. Lett. **6**, 57 (1961).
 - [15] E. E. Narimanov and A. D. Stone, Phys. Rev. B **57**, 9807 (1998).
 - [16] P. A. Dando, T. S. Monteiro, D. Delande, and K. T. Taylor, Phys. Rev. Lett. **74**, 1099 (1995).